A noncanonical PPARγ/RXRα-binding sequence regulates leptin expression in response to changes in adipose tissue mass

Yinxin Zhang[a,b], Olof Stefan Dallner[a], Tomoyoshi Nakadai[c], Gulya Fayzikhodjaeva[a,b], Yi-Hsueh Lu[a], Mitchell A. Lazar[d], Robert G. Roeder[c], and Jeffrey M. Friedman[a,b,1]

[a]Laboratory of Molecular Genetics, The Rockefeller University, New York, NY 10065; [b]Howard Hughes Medical Institute, The Rockefeller University, New York, NY 10065; [c]Laboratory of Biochemistry and Molecular Biology, The Rockefeller University, New York, NY 10065; and [d]Perelman School of Medicine, University of Pennsylvania, Philadelphia, PA 19104

Contributed by Jeffrey M. Friedman, May 15, 2018 (sent for review April 16, 2018; reviewed by Steven A. Kliewer, David J. Mangelsdorf, and Bruce M. Spiegelman)

Leptin expression decreases after fat loss and is increased when obesity develops, and its proper quantitative regulation is essential for the homeostatic control of fat mass. We previously reported that a distant leptin enhancer 1 (LE1), 16 kb upstream from the transcription start site (TSS), confers fat-specific expression in a bacterial artificial chromosome transgenic (BACTG) reporter mouse. However, this and the other elements that we identified do not account for the quantitative changes in leptin expression that accompany alterations of adipose mass. In this report, we used an assay for transposase-accessible chromatin with high-throughput sequencing (ATAC-seq) to identify a 17-bp noncanonical peroxisome proliferator-activated receptor gamma (PPARγ)/retinoid X receptor alpha (RXRα)-binding site, leptin regulatory element 1 (LepRE1), within LE1, and show that it is necessary for the fat-regulated quantitative control of reporter (luciferase) expression. While BACTG reporter mice with mutations in this sequence still show fat-specific expression, luciferase is no longer decreased after food restriction and weight loss. Similarly, the increased expression of leptin reporter associated with obesity in *ob/ob* mice is impaired. A functionally analogous LepRE1 site is also found in a second, redundant DNA regulatory element 13 kb downstream of the TSS. These data uncouple the mechanisms conferring qualitative and quantitative expression of the leptin gene and further suggest that factor(s) that bind to LepRE1 quantitatively control leptin expression and might be components of a lipid-sensing system in adipocytes.

leptin | adipose tissue | PPARγ/RXRα | weak binding | lipid sensing

Leptin is an adipocyte hormone that maintains homeostatic control of adipose tissue mass and functions as an afferent signal in a negative feedback loop. Leptin deficiency leads to extreme obesity in both mice and humans, while leptin treatment of wild-type mice reduces fat mass (1–7). Weight gain leads to an increased leptin level that, in turn, inhibits food intake and returns adipose tissue mass to the starting point. Similarly, weight loss decreases the leptin level, leading to increased food intake and increased fat mass. Thus, the quantitative changes in leptin expression associated with changes in nutritional state are critical for the proper functioning of this system. Consistent with this, the levels of leptin RNA and plasma leptin are highly correlated with adipocyte cell size and cellular lipid content (8–10). This has suggested that, analogous to a cholesterol sensing system in liver and other cell types (11, 12), there might be a lipid-sensing mechanism (or another mechanism, such as sensing of cell size) in adipocytes that adjusts the level of leptin gene expression to changes in the level of lipid stores. However, neither the molecular mechanisms controlling the change in leptin expression levels nor the elements of this putative signal transduction pathway are known (13).

To address this question, we initiated efforts to define *cis* elements and *trans* factors that control the quantitative expression of the leptin gene. Defining DNA sequence-binding sites has been crucial for identifying numerous transcription factors, including SP1 (14) and NF-κB (15). This approach is also analogous to that used to identify the aforementioned cholesterol-sensing system. In that case, studies of LDL receptor expression revealed that the levels of cholesterol in the endoplasmic reticulum membrane regulate cleavage and nuclear transport of the SREBP transcription factor, in turn, controlling the expression of genes that regulate cholesterol metabolism. However, analogous studies

Significance

Leptin gene expression is highly correlated with the lipid content of individual fat cells, suggesting that it is regulated by a "fat-sensing" signal transduction pathway. This possibility is thus analogous to the identification of a cholesterol-sensing pathway by studying the regulation of the LDL receptor gene by intracellular cholesterol. Several lines of investigation have suggested that, in addition to adipocytes, liver, neurons, and other cell types can sense changes in lipid content, although the molecular mechanisms are unknown. The data here provide a critical step toward elucidating the components of this putative system, which would be of great importance. These studies also identify a previously underappreciated role of the PPARγ/RXRα complex to regulate leptin expression.

Author contributions: Y.Z., R.G.R., and J.M.F. designed research; Y.Z., T.N., and G.F. performed research; O.S.D., Y.-H.L., and M.A.L. contributed new reagents/analytic tools; Y.Z. analyzed data; Y.Z. conceived/designed the study and performed the majority of the experiments; O.S.D. developed the strategy and reagents for generating bacterial artificial chromosome transgenic (BACTG) mice; T.N. performed the purification of PPARγ and RXRα proteins; G.F. performed pronuclear injections for BACTG mice and some of the in vivo luciferase imaging; Y.-H.L. made the leptin enhancer 1 (LE1) and LE2 reporters, worked with Y.Z. on the construction of the BAC reporter clones, and helped plan the studies using these reagents; M.A.L. helped perform the PPARγ ChIP-sequencing analysis; R.G.R. played a major role in planning the experiments, suggested the use of assay for transposase-accessible chromatin with high-throughput sequencing (ATAC-seq) instead of DNase-sequencing, suggested that leptin regulatory element 1 might be a weak PPARγ-binding site and provided purified protein to test this, provided a critical analysis of the data that were generated, and made many helpful suggestions; J.M.F. conceived the majority of the study; and Y.Z. and J.M.F. wrote the paper with input from all authors.

Reviewers: S.A.K., The University of Texas Southwestern Medical Center; D.J.M., The University of Texas Southwestern Medical Center; and B.M.S., Dana–Farber Cancer Institute and Harvard Medical School.

The authors declare no conflict of interest.

Data deposition: The data reported in this paper have been deposited in the Gene Expression Omnibus (GEO) database, https://www.ncbi.nlm.nih.gov/geo (accession no. GSE113413).

[1]To whom correspondence should be addressed. Email: friedj@mail.rockefeller.edu.

This article contains supporting information online at www.pnas.org/lookup/suppl/doi:10.1073/pnas.1806366115/-/DCSupplemental.

Published online June 11, 2018.

of leptin require that expression be monitored in vivo because cultured adipocytes, which have a very low lipid content, express an approximately 1,000-fold lower level of leptin RNA than do fat cells in vivo (16). Previous efforts to map *cis* elements controlling leptin expression have thus used bacterial artificial chromosome transgenic (BACTG) reporter animals with luciferase inserted at the transcription start site (TSS) of the leptin gene (17). Through a comprehensive deletion analysis, we previously found that a BACTG encompassing 31 kb (−22 to +8.8 kb) of the leptin locus showed fat-specific luciferase expression (18). Similar to the endogenous gene, luciferase expression was reduced after 48 h of food deprivation, while its expression was increased after crossing of the reporter mice to *ob*/*ob* mice that express very high levels of leptin RNA. We also found that a 3′ BACTG extending from −762 bp to +18 kb was able to drive reporter expression in a manner similar to the 5′ 31-kb (−22 to +8.8 kb) BACTG, while a BACTG extending from −762 bp to +8.8 kb lost fat-specific reporter expression. Subsequent studies have identified two redundant elements that can independently confer cell-specific expression of leptin in adipocytes: Leptin enhancer 1 (LE1) is localized between −16.5 and −16.1 kb upstream of the leptin TSS, while LE2 is located between +13.6 and +13.9 kb downstream of the leptin TSS. However, because deletion of these elements ablates fat-specific expression altogether, it is not possible to assess the role of these specific sequences to quantitatively regulate leptin expression. Similarly, while other factors, including C/EBP**α** and SP1 (19, 20), FOSL2 (21), and NFY (18), have been reported to play a role in leptin expression, none have been shown to quantitatively regulate this gene.

In this report, we employed the assay for transposase-accessible chromatin with high-throughput sequencing (ATAC-seq) (22) as part of an unbiased screen to identify sites of transcription factor binding in inguinal white adipose tissue (iWAT) from fed, food-restricted (48 h), and *ob*/*ob* mice. Deep sequencing revealed a highly conserved noncanonical footprint for a PPARγ/RXRα-binding site within LE1 [referred to hereafter as leptin regulatory element 1 (LepRE1)] in adipose tissue nuclei derived from *ob*/*ob* mice, but not from adipose tissue of wild-type mice. Point mutations in this regulatory sequence in the 5′ reporter BACTG (−22 to +8.8 kb) abrogated quantitative regulation of luciferase in adipose tissue from fasted and obese mice. A functionally equivalent PPARγ/RXRα-binding site was also found within LE2, potentially explaining the functional redundancy of these elements. Purified PPARγ/RXRα binds weakly to these sequences, and both gain-of-function and loss-of-function mutations within the core sequence affect the regulated expression of the reporter. In addition, mutations in the adjacent PPARγ extension site disrupt the proper quantitative control of reporter expression. These data suggest a model in which the quantitative regulation of leptin expression depends on the stabilization of PPARγ/RXRα binding to an otherwise weak binding site by an accessory factor binding to the adjacent extension site.

Results

A Fat-Regulated Footprint, LepRE1, Is a Noncanonical PPARγ/RXRα-Binding Site. To find potential LepREs that respond to changes in fat mass, we isolated nuclei from inguinal iWAT of fasted, fed, and *ob*/*ob* mice and generated genome-wide footprints using ATAC-seq. In this method, isolated nuclei are incubated with a hyperactive transposase loaded with adaptor sequences so that DNA sequences from open regions of chromatin (i.e., DNase-hypersensitive regions) can be PCR-amplified using the adaptor sequences as primers. Deep sequencing of the PCR products yields a genome-wide inventory of sequences from accessible regions of chromatin (22). Furthermore, analysis of the heights of the peaks of the DNA sequence reads reveals DNA footprints indicative of protein binding. Using this method, we identified six peaks within −22 to +8.8 kb of the leptin gene that showed a threefold or higher signal in adipose tissue nuclei from *ob*/*ob* mice compared with nuclei from fed and fasted mice (Fig. 1*A*). These six peaks included the aforementioned LE1 between −16.5 and −16.1 kb of the TSS, the proximal promoter around the TSS, and four regions within the first intron. The differences in access of the transposase to the proximal promoter and the transcribed regions in the first exon are consistent with the higher level of expression of this gene in *ob* vs. wild-type adipose tissue.

We thus focused on the LE1 sequence at ∼−16 kb because it is not transcribed and also because a 400-bp deletion of LE1 in a BACTG (−22 to +8.8 kb) abolishes fat-specific expression of a luciferase reporter. Within LE1, there is a 101-bp segment (mm9, chr6: 28993757–28993857) that is almost identical among 20 placental mammal species, which is consistent with the finding that fat-specific expression of leptin is only evident in mammals (23). Within this 101-bp region of LE1, there is a small 17-bp footprint in *ob*/*ob* but not wild-type adipose tissue nuclei. The

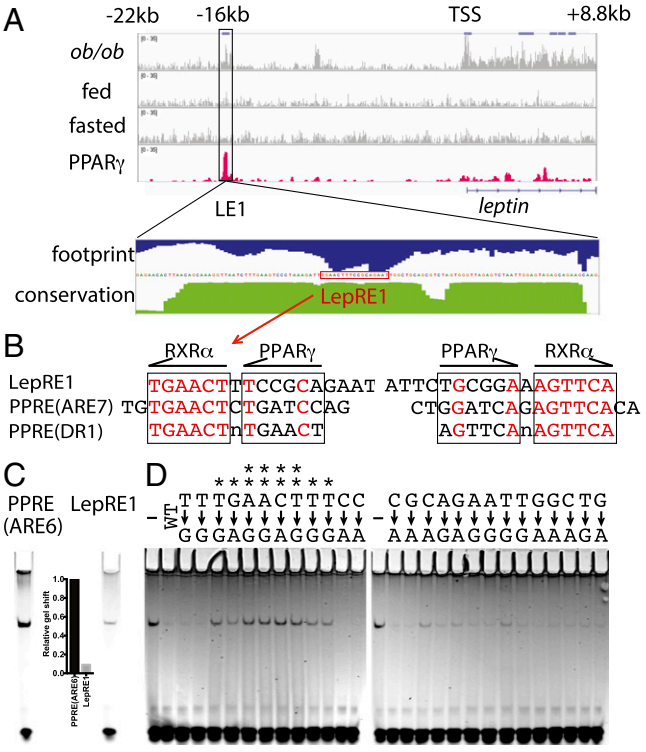

Fig. 1. Fat-regulated footprint, LepRE1, is a noncanonical PPARγ/RXRα-binding site. (*A*) ATAC-seq was performed using nuclei from the inguinal fat of *ob*/*ob*, fed, and fasted B6 mice and compared with PPARγ ChIP-seq in the inguinal fat from B6 mice (32, 33). Data for sequences between −22 and +8.8 kb of the leptin gene locus are shown. Regions with a threefold change from *ob*/*ob* mice vs. fasting are highlighted. The −16-kb region of the leptin gene is enlarged to show the calculated footprint score (blue) and conservation score within mammals (green). The LepRE1 sequence is denoted by a red box. (*B*) Sequence alignment of LepRE1, PPRE (ARE7), and PPRE (DR1). (*Left*) LepRE1 sequence denoted by the red box in *A* is shown. The nucleotides that are conserved between the PPREs and LepRE1 are colored red. The PPARγ- and RXRα-binding sequences are boxed based on the solved crystal structure (40). (*C*) EMSA of purified PPARγ/RXRα with IRDye 700-labeled PPRE (ARE6) and LepRE1 oligos. The shifted bands were quantified with ImageStudioLite and normalized to PPRE (ARE6). (*D*) EMSA competition studies of excess unlabeled wild-type (WT) LepRE1 oligos or oligos with scanned point mutations with IRDye 700-labeled WT LepRE1 in the presence of purified PPARγ/RXRα. * indicates point mutation in LepRE1 that affects the binding to purified PPARγ/RXRα proteins; ** indicates point mutation in LepRE1 that abolishes the binding to purified PPARγ/RXRα proteins.

footprint showed two apparent peaks, suggesting that two (or more) proteins bound there. We refer to this footprinted sequence as LepRE1 (Fig. 1*A*).

We noticed that six consecutive base pairs (out of 13) of the footprinted sequence of LepRE1 were identical to the RXRα-binding sequence [referred to as the conserved direct repeat 1 (DR1) half-site] of the Fabp4/aP2 gene enhancer. This binding site is referred to as the peroxisome proliferator response element (PPRE)/adipocyte regulatory factor response element 7 (also known as ARE7), and this binding site is composed of a direct repeat of two DR1 half-sites with a 1-nt spacer (24, 25) (Fig. 1*B*). PPARγ, a member of the nuclear hormone receptor superfamily, is the master regulator of adipogenesis (26, 27). This transcription factor binds as a heterodimer with RXRα, another nuclear receptor, to a DR1 sequence (28). However, in LepRE1, the next 6-bp sequence, 3′ to the conserved DR1 (i.e., the second half-site), had only very limited homology to DR1 as would typically be found in a canonical PPARγ-binding sequence or PPRE.

Thus, the footprint we found in the −16-kb upstream region of the leptin gene is not a canonical PPRE (DR1) in that a single DR1 half-site was followed by a nonhomologous sequence (Fig. 1*B* and *SI Appendix*, Fig. S1*A*). Indeed, because of this, none of the current algorithms that identify DNA-binding sites identified LepRE1 as a PPARγ/RXRα-binding sequence at all. However, as shown below, this sequence can bind to a PPARγ/RXRα heterodimer, albeit more weakly than does a canonical binding site.

We confirmed that the PPARγ/RXRα protein complex could bind to this sequence using an EMSA assay in which purified PPARγ and RXRα were incubated with LepRE1 oligonucleotides labeled with infrared dye (IRDye) 700. FLAG-tagged mouse PPARγ2 and human RXRα proteins were purified from baculovirus-infected Sf9 cells. We found that the purified protein bound to this sequence with an affinity one-tenth that of a canonical DR1 PPRE. In these studies, we used the ARE6-binding site rather than the aforementioned ARE7-binding site because more extensive mutagenesis has been performed for this sequence (24) (Fig. 1*C*). ARE6 and ARE7 share six of 13 core DR1 nucleotides, and both provide high-affinity sites for PPARγ binding to the Fabp4/aP2 enhancer (25). This gel shift was abolished after coincubation with an excess of unlabeled wild-type DNA fragments, while unlabeled DNA fragments with point mutations in the RXRα-binding sequence, particularly the AACT/AGTT part of the conserved DR1 half-site of LepRE1, no longer competed with the labeled probe in the gel shift (Fig. 1*D*). In contrast, unlabeled DNA fragments with point mutations in the sequences 3′ to the conserved DR1 half-site and the PPARγ-binding sequence (TCCGCA/TGCGGA) as well as mutations in the extension sequence for PPARγ (Fig. 1*D*) competed for binding in a similar manner to wild-type oligonucleotides. The extension sequence is adjacent to the nonconserved half-site with the sequence GAAT/ATTC. It previously has been suggested that this site binds other transcription factors, the identities of which have not been determined (29). These results show that the RXRα-binding portion of LepRE1 is required for the (weaker) binding of PPARγ/RXRα to this sequence (Fig. 1*D*). These in vitro EMSA findings are also consistent with data from ChIP-sequencing (ChIP-seq) analyses identifying sites of PPARγ binding (30–33) (Fig. 1*A* and *SI Appendix*, Fig. S1*B*). These data confirm that PPARγ/RXRα weakly binds to LepRE1 in adipocyte nuclei in vivo via interactions with a noncanonical PPARγ-binding site.

A 3′ Fat-Regulated Footprint, LepRE2, Is Homologous to LepRE1. LE1, located between −16.5 and −16.1 kb, and LE2, located between +13.6 and +13.9 kb, are redundant elements that can independently confer qualitative and quantitative expression of luciferase in leptin reporter mice, raising the possibility that functionally similar elements at both sites can regulate the level of leptin gene expression (18). In previous studies, deletion of LE2 in a BACTG extending between −0.762 and +18 kb ablated fat-specific expression of a luciferase reporter. We thus used ATAC-seq to identify open regions of chromatin within the −0.762 to +18-kb region of the leptin gene and found 10 hypersensitive peaks with a threefold difference between *ob*/*ob* and fasted mice. All but one of these 10 peaks were in transcribed regions that included the proximal promoter around the TSS and four regions within the first intron (referred to previously), as well as one region within the second intron, two regions within the third exon, one region around the transcription termination site, and one region downstream of the transcription termination site.

The only site from a nontranscribed region was found immediately after the transcription termination site, and showed a highly significant peak in *ob*/*ob* adipocyte nuclei in a 66-bp segment of LE2 (mm9, chr6: 29023967–29024032). As was also the case for LepRE1, this sequence was conserved among 20 placental mammal species (Fig. 2*A*). The ATAC-seq data identified a small footprint within this 66-bp segment referred to as LepRE2 (Fig. 2*A*). LepRE2 was identical to LepRE1 at 10 (59%) of 17 nucleotides (Fig. 2*B*). Among the 10 identical nucleotides between LepRE1 and LepRE2, four (ATTC/GAAT) were in the 5′ extension sites of PPARγ, while five (GAAAG/CTTTC) of the other six were in the middle of the PPARγ/RXRα-binding site (Fig. 2*B*). Although the sequence LepRE2 did not contain a single conserved DR1 half-site sequence as in LepRE1, LepRE2 had the same DNA sequence (AAAGG/CCTTT) as a central portion of a consensus DR1 motif, as shown in the analyses of genome-wide PPARγ ChIP-seq and RXRα ChIP-seq data (30, 31) (*SI Appendix*, Fig. S1*A*). Like LepRE1, current algorithms that identify DNA-binding sites did not designate this LepRE2 sequence as a PPARγ/RXRα-binding sequence. Purified PPARγ/RXRα complex bound to this sequence, as shown by EMSA (Fig. 2*C*). However, similar to LepRE1, the binding affinity of the purified PPARγ/RXRα complex to an IRDye 700-labeled LepRE2 oligonucleotide was also weak, with an approximately fivefold lower signal compared with that observed for binding to a typical PPRE (ARE6). The binding site of the PPARγ/RXRα complex was further refined by testing the ability of excess unlabeled wild-type oligonucleotides and oligonucleotides with mutations in each of the positions in LepRE2 to compete with the labeled oligonucleotide binding to PPARγ/RXRα (Fig. 2*D*). Oligonucleotides with point mutations in the central part of the DR1 ChIP-seq motif (AAAGG/CCTTT) no longer competed with the gel shift band, while mutations in other segments that included the extension sequence showed a similar ability as wild-type oligonucleotides to compete for binding. Similar to LE1/LepRE1, the LE2/LepRE2 peak was also identified in several published PPARγ ChIP-seq datasets (32, 33), indicating binding of this transcription factor to the leptin gene in adipocytes in vivo (Fig. 2*A* and *SI Appendix*, Fig. S1*B*).

Fat-Specific Expression in Reporter Mice with LepRE1 Mutations. Previous studies have shown that PPARγ, at least by itself, is not sufficient to induce a high level of leptin expression. For example, leptin expression is extremely low in cultured adipocytes and in brown fat despite the fact that they express high levels of this transcription factor (16). To confirm that LepRE1 and LepRE2 are functional PPREs, we cotransfected PPARγ and RXRα into HEK293T cells expressing a luciferase reporter construct. We found that PPARγ and RXRα can indeed activate the LE1 and LE2 enhancers upstream of a luciferase reporter with an ∼10-fold induction relative to control experiments without cotransfection of PPARγ and RXRα (Fig. 3*A*). Interestingly, treatment with the RXR ligand 9-*cis*-Retinoic acid decreases the LE1-driven and LE2-driven luciferase activity. The PPARγ ligand rosiglitazone also decreases reporter expression, although to a lesser extent than 9-*cis*-Retinoic acid (Fig. 3*A*). These results are

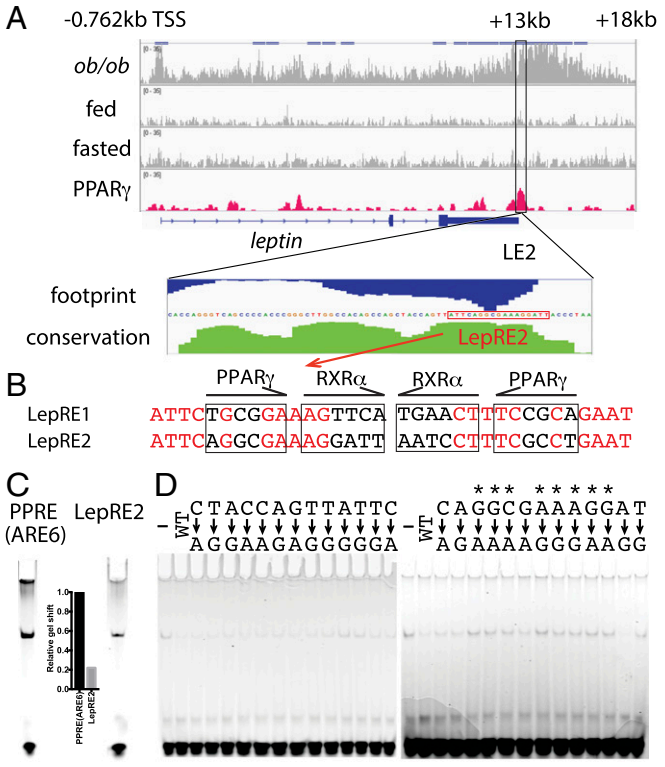

Fig. 2. A 3′ fat-regulated footprint, LepRE2, is homologous to LepRE1. (*A*) ATAC-seq results of the inguinal fat from *ob/ob* fed and fasted B6 mice, and PPARγ ChIP-seq in the inguinal fat from fed B6 mice (32, 33) between −0.762 and +18 kb sequences of the leptin locus are shown. Regions with a threefold change in nuclei from *ob/ob* vs. fasted mice are highlighted. The +13-kb region of the leptin gene is enlarged to show the calculated footprint score (blue) and conservation score within mammals (green). The LepRE2 sequence is denoted by a red box. (*B*) Sequence comparison of LepRE1 and LepRE2. (*Left*) LepRE2 sequence denoted by the red box in *A* is shown. The conserved nucleotides are colored red. PPARγ- and RXRα-binding sequences are boxed based on the solved crystal structure (40). (*C*) EMSA of purified PPARγ/RXRα with IRDye 700-labeled PPRE (ARE6) and LepRE2 oligos. The shifted bands were quantified with ImageStudioLite and normalized to PPRE (ARE6). (*D*) EMSA competition studies of excess unlabeled wild-type (WT) LepRE2 and oligos with point mutations using IRDye 700-labeled WT LepRE2 in the presence of purified PPARγ/RXRα. * indicates point mutation in LepRE2 that affects the binding to purified PPARγ/RXRα proteins.

consistent with the finding that thiazolidinediones inhibit leptin expression (34–36).

We thus investigated whether this noncanonical PPARγ/RXRα-binding site is required for proper qualitative and quantitative expression of leptin by making point mutations in LepRE1 in the reporter BACTG that extends from −22 to +8.8 kb. In this BACTG, luciferase is inserted by homologous recombination into the TSS. Three LepRE1 mutants were characterized: (*i*) a gain-of-function PPARγ/RXRα-binding mutant LepRE1 (GOF) DR1, in which a canonical DR1 half-site has replaced the second noncanonical 3′-binding site; (*ii*) a loss-of-function PPARγ/RXRα-binding mutant LepRE1 (LOF) in which a point mutation was introduced into the highly conserved DR1 half-site sequence (i.e., the RXRα-binding region that is required for binding) (Fig. 1*D*); and (*iii*) an extension mutant LepRE1 (EXT) in which a point mutation was introduced in the 5′ flanking sequence upstream of the core DR1. As mentioned, previous studies suggest the 5′ extension site of PPARγ may be a target of other binding proteins (29). EMSA assays confirmed that the DR1 GOF mutant bound to purified PPARγ/RXRα more strongly than did the wild-type sequence, that the LOF mutant failed to bind, and that the EXT mutant bound with similar affinity to the wild-type oligonucleotide (Fig. 3*B*).

We next made multiple BACTG reporter lines for each of the three different LepRE1 mutants. All of the lines for the GOF DR1, LOF, and EXT mutants expressed leptin luciferase reporter exclusively in adipose tissue, albeit with lower baseline levels of expression vs. the wild-type reporter mice. In temporal analyses (*SI Appendix*, Fig. S2), we also noticed a progressive diminution in luciferase expression between 3 and 8 wk of age, with the relative level of luciferase expression in the LepRE1 DR1 reporter mice decreasing from 120% of the wild-type BACTG to 20~30% that of the control construct by 8 wk of age, after which time the expression level was stable. At baseline, the level of luciferase expression in the LepRE1 LOF reporter mice was fat-specific but expressed at a considerably lower level of ~4–8% that of the wild-type construct. Finally, luciferase expression in the LepRE1 EXT

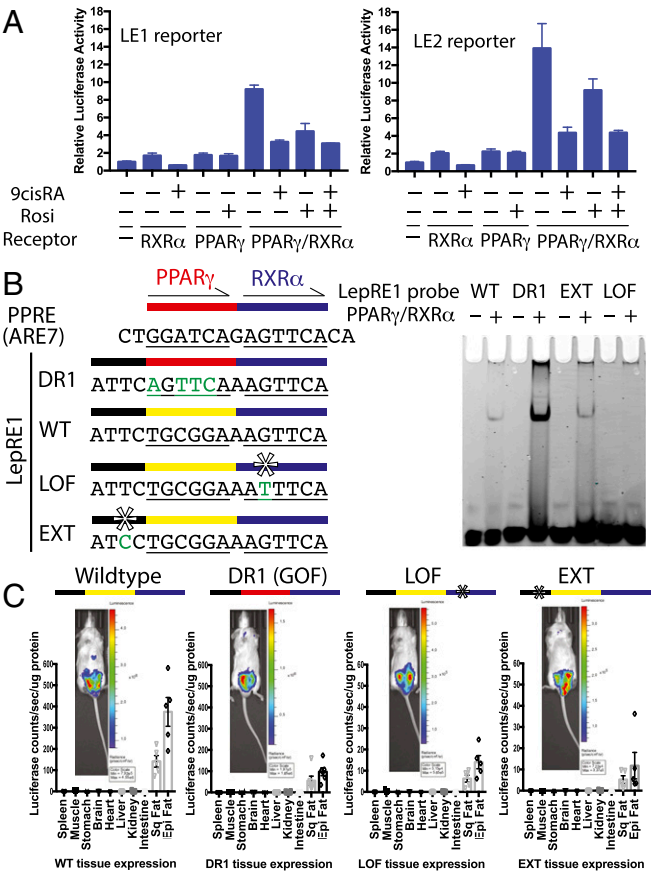

Fig. 3. Fat-specific expression in reporter mice with LepRE1 mutations. (*A*) PPARγ/RXRα complex activates both LE1 and LE2 enhancers in transfected HEK293T cells in a dual-luciferase reporter assay. (*B*) Series of point mutations were introduced into LepRE1 for functional studies in vitro and in vivo. Sequence alignment of PPRE (ARE7), a LepRE1 DR1 GOF mutation, wild-type (WT) LepRE1, a LepRE1 LOF mutation, and an EXT mutant in the LepRE1 extension site. The mutated nucleotides are colored green, and an asterisk marks the sites of the mutations. A red line above the sequence indicates the canonical PPARγ-binding region, while a yellow line shows noncanonical PPARγ binding. The blue line shows RXRα binding. The black line represents the 5′ extension sequence. (*Right*) EMSA results of LepRE1 WT, DR1, LOF, and EXT with purified PPARγ/RXRα. (*C*) These point mutations were then introduced into leptin luciferase reporter mice that extended between −22 and +8.8 kb of the leptin locus. Luciferase expression is shown for BACTG mice with the WT, DR1, LOF, and EXT LepRE1 sequences. Ten tissues were dissected and processed for protein quantification and luciferase measurement. A representative IVIS mouse image is also shown for each transgenic line.

reporter mice was ∼15% that of the wild-type reporter and decreased to a level ∼4% that of the wild-type reporter mice between 3 and 8 wk of age (*SI Appendix*, Fig. S2). These data show that the newly identified noncanonical PPARγ/RXRα-binding site is necessary for normal levels of expression of the leptin gene. As mentioned, luciferase was expressed exclusively in adipose tissue in all cases and the level of luciferase expression was stable in all three lines after 8 wk. Thus, all subsequent experiments were performed in mice that were 9 to 13 wk of age (Fig. 3*C*). We next evaluated the impact of the PPARγ/RXRα-binding site mutations on the level of reporter expression after a period of food restriction or in obese animals.

Dysregulation of Leptin Reporter Expression After Weight Loss and Weight Gain. Weight loss after a period of food restriction is associated with a decrease in leptin gene expression and leptin plasma level. After 2 d of food restriction, similar to expression of the endogenous gene, expression of the leptin luciferase reporter in the 5′ wild-type BACTGs (−22 to +8.8 kb) decreased 3.3-fold (3.1×10^8 p·s^{-1} units of total flux) relative to the average expression level before fasting (Fig. 4*A*). In contrast, the level of luciferase expressed from the GOF mutant (with the stronger PPARγ/RXRα-binding site, LepRE1 DR1) did not decrease after 2 d of food restriction. Similarly, the reporter animals with a point mutation in the 5′ extension site (LepRE1 EXT) also showed a stable level of luciferase expression after a fast. Importantly, as shown previously (Fig. 3*B*), this mutation in the extension sequence did not alter the binding of PPARγ/RXRα to LepRE1. Finally, the reporter animals with a loss of function of PPARγ/RXRα binding (LepRE1 LOF) showed a 1.6-fold decrease of luciferase expression after fasting [1.1×10^7 p·s^{-1} (total flux)], and the magnitude of this decrease was 27.7-fold lower than that seen in wild-type mice after 2 d of food restriction (Fig. 4 *A* and *B*). The body weight and fat mass of each of the groups (11–13 wk old) was the same, showing that the altered reporter expression was not a result of differences in adipose tissue mass (Fig. 4*C*).

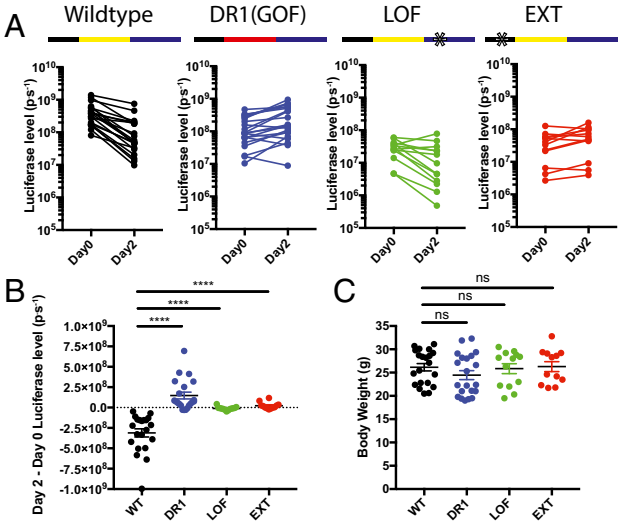

Fig. 4. Dysregulation of leptin reporter expression after weight loss. (*A*) Individual whole-body luciferase levels before fasting (day 0) and after 2 d of fasting (day 2) for the wild-type leptin BACTG mouse (−22 to +8.8 kb) and the DR1 (GOF), LOF, and EXT mutants are shown. The mice were between 11 and 13 wk old. (*B*) Difference between day 2 and day 0 whole-body luciferase level (Day 2−Day 0) for individual mice is shown. WT, wild type. (*C*) Body weight for corresponding individual mice on day 0. In *A*–*C*, WT ($n = 21$), DR1 ($n = 21$), LOF ($n = 13$), EXT ($n = 12$). ns, $P > 0.05$. ****$P < 0.0001$.

We next analyzed the effect of these mutations on reporter expression in obese animals by mating the aforementioned reporter lines to *ob*/*ob* mice. The *ob*/*ob* mice carry a mutation in the leptin coding sequence and show a dramatic compensatory increase in the level of expression of leptin RNA. As above, no significant differences in body weight were observed in the mutant reporter animals vs. mice carrying the wild-type reporter (Fig. 5*A*). Nine-week-old *ob*/*ob* mice had an average body weight of 42 g, which is significantly higher than the 21-g average body weight in 9-wk-old *ob*/$^+$ mice. As previously reported, the level of the luciferase reporter was 9.6-fold higher [7.6×10^9 p·s^{-1} (total flux)] in *ob*/*ob* transgenic animals expressing the wild-type reporter relative to the level of reporter expression in nonobese *ob*/$^+$ mice.

In contrast, and relative to control mice, the increase in the levels of luciferase expression in 9-wk-old *ob*/*ob* mice carrying the LOF reporter was 20.6-fold lower [3.7×10^8 p·s^{-1} (total flux)] than the increase in 9-wk-old *ob*/*ob* mice carrying the wild-type reporter. Similarly, in *ob* animals carrying the EXT reporter construct, the increase of luciferase expression in *ob*/*ob* mice was 15.8-fold lower [4.8×10^8 p·s^{-1} (total flux)] than the increase in luciferase expression in *ob*/*ob* mice with the wild-type reporter (Fig. 5 *B* and *C*).

We found that the increased luciferase expression with obesity was impaired (albeit to a lesser extent) in the DR1 BACTG reporter mice, as the increased expression [3.9×10^9 p·s^{-1} (total flux)] of this reporter construct in *ob*/*ob* mice was 1.9-fold lower than the expression in *ob*/*ob* mice from the wild-type construct (Fig. 5 *B* and *C*). To reconfirm that the induction of luciferase expression from the LepRE1 DR1 reporter line was impaired, a second cohort of 11-wk-old animals was analyzed. Eleven-week-old *ob*/*ob* and *ob*/$^+$ mice had average body weights of 49 g and 25 g, respectively. While the body weights of the LepRE1 wild-type and DR1 *ob*/*ob* animals were similar, the increase in luciferase expression from the DR1 reporter [5.3×10^9 p·s^{-1} (total flux)] was 1.7-fold lower than the increase in expression from the wild-type reporter [9.1×10^9 p·s^{-1} (total flux)] (*SI Appendix*, Fig. S3).

Finally, we tested whether additional factors in a nuclear extract from *ob*/*ob* adipose tissue can interact with the PPARγ/RXRα:LepRE1 complex. We found that addition of a nuclear extract from *ob*/*ob* adipocyte supershifted the PPARγ/RXRα:LepRE1 complex in an EMSA assay, while nuclear extracts from wild-type adipose tissue did not (*SI Appendix*, Fig. S4).

In summary, while leptin reporter mice with mutations in LepRE1 show fat-specific expression of luciferase (albeit with lower baseline levels), all three mutants show an impaired response to nutritional changes. The DR1 and EXT mutations fail to reduce luciferase expression after fasting and also show an impairment in the increased expression normally seen on an *ob*/*ob* background. The LOF BACTG reporter mice show a lesser reduction of reporter expression after weight loss and also show a profound defect in the increase of luciferase expression with obesity. Overall, these data suggest that *trans* factors binding to this noncanonical PPARγ-binding site and the adjacent EXT sequence play a critical role in controlling the quantitative expression of the leptin gene.

Discussion

Quantitative control of leptin expression is critical for the homeostatic control of adipose tissue mass. However, neither the transcription mechanism nor the signal transduction pathway that regulates the level of leptin expression is known. Their elucidation has been confounded by the finding that the key regulatory elements regulating leptin expression appear to be responsible for its tissue-specific expression in fat. We thus sought to identify transcription factor-binding sites whose footprints (reflecting occupancy) differed in obese vs. wild-type animals (Fig. 1*A*). Here, we report the identification and functional characterization of a specific PPARγ-binding site (LepRE1) that is responsible

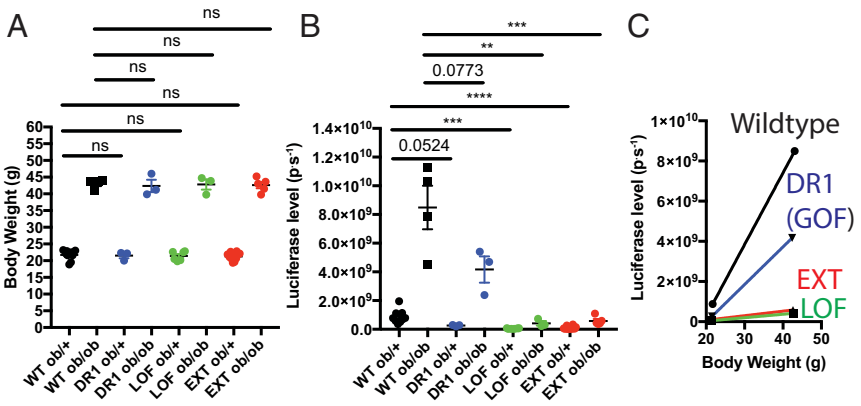

Fig. 5. Dysregulation of leptin reporter expression after weight gain. (*A*) Body weight for individual 9-wk-old *ob*/$^{+}$ or *ob*/*ob* BACTG mice. (*B*) Corresponding whole-body luciferase level for individual 9-wk-old *ob*/$^{+}$ or *ob*/*ob* mice is shown. (*C*) Average luciferase level relative to body weight of *ob*/$^{+}$ vs. *ob*/*ob* mice is shown for each of the constructs. A diagram for each sequence is shown. In *A*–*C*, wild-type (WT) *ob*/$^{+}$ ($n = 9$), WT *ob*/*ob* ($n = 4$), DR1 *ob*/$^{+}$ ($n = 3$), DR1 *ob*/*ob* ($n = 3$), LOF *ob*/$^{+}$ ($n = 6$), LOF *ob*/*ob* ($n = 3$), EXT *ob*/$^{+}$ ($n = 10$), EXT *ob*/*ob* ($n = 5$). ns, $P > 0.05$. $^{**}P < 0.01$; $^{***}P < 0.001$; $^{****}P < 0.0001$.

for the quantitative control of the leptin gene without affecting its fat-specific expression.

Previous studies from our laboratory have shown that redundant sequences in the extreme 5′ and 3′ regions of the gene, greater than 10 kb from the TSS, can confer fat-specific expression of the leptin gene (18). However, because mutations in these regions interfered with the fat-specific expression of this gene, it was impossible to define the sequences that quantitatively regulated leptin expression. This problem also applied to studies of other transcription factors, including C/EBPα and SP1 (19, 20), FOSL2 (21), and NFY (18), each of which has been reported to play a role in tissue-specific leptin expression in adipose tissue. Thus, in contrast to the binding sites for these other factors, LepRE1 and the factors that bind to it uncouple the mechanisms conferring quantitative expression of the leptin gene from its fat-specific expression.

LepRE1 and a functionally redundant element in the 3′ region of the leptin gene (LepRE2, Fig. 2) show weak binding to PPARγ, raising the possibility that an additional stabilizing factor is necessary for its binding. PPARγ binding to the LepRE1 and LepRE2 sites is not seen in macrophages (33) (*SI Appendix*, Fig. S1), adding further evidence that there is an accessory factor that enables binding in adipocytes. PPARγ, forming an obligate heterodimer with RXRα, is a master regulator of adipogenesis (26, 27). PPARγ expression is highly correlated with leptin expression (37), and an adipose-specific PPARγ deletion reduces leptin expression, although this reduction is thought to be secondary to a defect in lipoatrophy (38). However, PPARγ by itself is not sufficient for a high level of leptin expression. For example, leptin expression is extremely low in cultured adipocytes despite the fact that they express high levels of this transcription factor (16). In addition, thiazolidinediones were found to inhibit leptin expression despite activating PPARγ in cultured adipocytes and rodents (34–36).

The finding of a noncanonical PPARγ/RXRα-binding sequence (LepRE1) and the effect of cognate mutations in impairing the nutritional regulation of the leptin gene provide evidence that an additional factor(s) is necessary for PPARγ-regulated expression. The canonical PPARγ/RXRα-binding PPRE motif known as the DR1 sequence is a strong target for binding of this transcription factor (28). The LepRE1 contains an RXRα-binding sequence identical to that in the PPRE (ARE7), but the other half is diverged (Fig. 1*B*). This alteration explains why this sequence was not identified as a binding site by current algorithms. These sequence changes also render the PPARγ/RXRα binding much weaker and explain why PPARγ alone is not sufficient to induce a high level of leptin expression in cultured adipocytes. Furthermore, a PPARγ ligand, rosiglitazone (and an RXRα ligand, 9-*cis*-Retinoic acid), decreases the expression of both LE1-driven and LE2-driven luciferase activity (Fig. 3*A*). Such results could explain why thiazolidinediones inhibit leptin expression despite being thought of as PPARγ agonists. These data are also consistent with previous results with the estrogen receptor, where ligands can reduce expression of a target gene in the absence of a functional coactivator (39). While there were other potential noncanonical PPARγ/RXRα-binding sites in the LE1 region, LepRE1 is the only one that was identified in the footprinting studies using ATAC-seq. Nonetheless, even though the LepRE1 site was functionally validated and found to be necessary, as mentioned above, it is still possible that other sites could also contribute.

A functional requirement of the PPARγ/RXRα complex for quantitative transcriptional regulation of leptin by binding to LepRE1 is suggested by the following evidence: (*i*) Purified PPARγ/RXRα proteins bound IRDye 700-labeled LepRE1 with sequence specificity in an (in vitro) EMSA assay (Fig. 1 *C* and *D*); (*ii*) ChIP-seq analysis identified PPARγ binding to LepRE1 in vivo (30–33) (Fig. 1*A* and *SI Appendix*, Fig. S1*B*); (*iii*) at baseline, the level of luciferase expression in the LepRE1 LOF reporter mice was considerably lower, with a fat-specific luciferase expression level 4∼8% that of the wild-type construct (Fig. 3 and *SI Appendix*, Fig. S2); and (*iv*) the LOF BACTG reporter mice showed a lesser reduction of reporter expression after fasting and an impairment in the increase of luciferase expression in *ob*/*ob* animals (Fig. 5).

As mentioned above, these data suggest that an additional factor is required to stabilize PPARγ binding to this site to regulate the quantitative level of leptin expression. Our data further suggest that this putative accessory factor binds to the adjacent extension sequence (and potentially part of the nearby DR1 half-site for PPARγ) because mutations in this sequence (LepRE1 EXT) and the nearby PPARγ-binding sequence (LepRE1 DR1) do not alter the specificity of reporter expression in fat but do impair the effect of fasting or obesity. The mutation in the extension sequence also dramatically decreases the baseline level of reporter expression, further suggesting that it provides a binding site for a factor that is necessary for high-level expression of leptin in vivo. We also noticed that fat nuclear extracts from *ob*/*ob* mice can supershift a purified PPARγ/RXRα:LepRE1 complex in an EMSA assay (*SI Appendix*, Fig. S4), suggesting that an additional factor(s) in *ob*/*ob* adipocytes is part of the complex. Efforts to identify this other factor(s) are

underway. However, we have not ruled out the possibility that a conformational change in PPARγ itself could potentially affect its binding to the extension site as the PPARγ DNA-binding domain includes a C-terminal helix that inserts into the minor groove of this extension sequence (as shown in the PPARγ/RXRα cocrystal structure) (40). There are numerous other instances in which gene expression is controlled by the stabilization of weak binding. For example, *Escherichia coli* RNA polymerase alone binds fairly weakly to the classic *lac* promoter and requires cooperative binding with another low-affinity partner (cAMP-CAP) for high-level expression of β-galactosidase in the absence of glucose (41). The requirement for accessory factors to facilitate PPARγ-mediated gene expression also has a precedent in brown fat (42). Brown fat expresses high levels of PPARγ but does not express UCP1 unless the PGC-1 coactivator is also expressed, although activation of the UCP1 promoter in brown fat also involves other factors such as PRDM16, MED1, and HDAC3 (33, 43, 44). Thus, the stabilization of PPARγ at a noncanonical site may provide a general mechanism for the control of a wide array of other PPARγ target genes. Indeed, previous studies have suggested that the 5′ extension site of PPARγ in the classic DR1 motif may indeed be involved in binding to other factors (29). Structural studies of the glucocorticoid receptor haves shown how coregulatory proteins can alter transcription factor conformation and sequence selection (45). The nature of the accessory factor regulating leptin expression is unknown and under intense investigation. It is noteworthy that while the RXRα-binding sequences are identical between LepRE1 and PPRE (ARE7) of the Fabp4/aP2 gene, LepRE1 has a unique 5′ extension sequence that differs from the extension sequence of the PPARγ site that regulates the UCP1 gene.

We found an impairment in the decrease in reporter expression from the LepRE1 mutants after fasting, as well as a markedly diminished absolute increase in reporter expression from all three LepRE1 mutants after breeding to *ob/ob* mice. However, there was still a small relative increase in the expression from the LOF and EXT reporter constructs with obesity (Fig. 5*C*). This suggests that there may exist additional pathways that can partially up-regulate leptin transcription in *ob/ob* mice. This may be similar to the compensatory increase of leptin transcription from wild-type mice to *ob*/$^{+}$ mice. Because the body weight difference between wild-type and *ob*/$^{+}$ mice is almost indistinguishable, this additional LepRE1-independent pathway may not be associated with lipid content in fat.

The most parsimonious model to explain our findings is that the quantitative or qualitative state of an accessory factor(s) that binds to the extension site is altered in concert with changes in fat mass (or something that correlates with these changes) and, in turn, regulates the binding of PPARγ/RXRα binding to LepRE1, thus controlling transcription of the leptin gene (Fig. 6). The identification of this factor could thus potentially illuminate the nature of the adipocyte signal transduction pathway that is responsible for the regulated expression of leptin in parallel with changes in cellular lipid content. While several lines of evidence have suggested that cellular lipid content is sensed in adipocytes, the cellular mechanisms are not known. Lipid sensing has also been invoked as potentially regulating the activity of hypothalamic neurons and hepatic metabolism, although the underlying mechanism in these cell types is similarly unknown (46). Possible mechanisms could include regulation of a lipid metabolite, sensing of cell size (which would increase as lipid accumulates), effects of oxygen (the partial pressure of which could vary based on the distance of the nucleus from the capillaries), or other mechanisms. This mystery is analogous to the cholesterol-sensing problem for cells, which was resolved by defining the regulatory mechanisms and signal transduction pathway that regulates the transcription of LDL receptor (11, 12, 47, 48). Identification of the putative accessory factors that bind to the noncanonical PPARγ/RXRα site that we have implicated in the regulation of leptin expression could help resolve this conundrum and lead to the identification of the signal transduction mechanism that links changes in cellular lipid content, or its surrogate, to changes in gene expression and possibly other cellular functions. A deeper understanding of this putative lipid-sensing mechanism could be of general importance for understanding the mechanisms responsible for nutritionally mediated changes in cell function and gene expression.

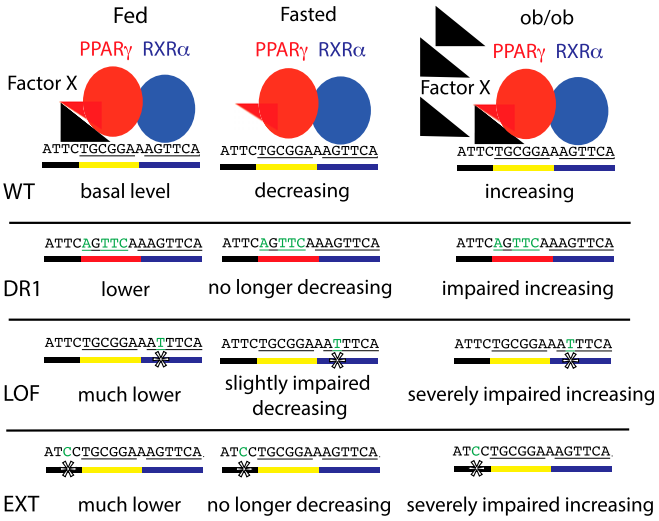

Fig. 6. Summary of leptin reporter mice with LepRE1 mutations and model for the transcriptional regulation of leptin through a weak PPARγ/RXRα-binding site, LepRE1. The data support a model in which PPARγ/RXRα (red and blue) binding to LepRE1 is stabilized by another factor (black triangle). The mutated nucleotides are green, and an asterisk marks the mutations. A red line below the sequence indicates the canonical PPARγ-binding site, while a yellow line shows noncanonical PPARγ binding. A blue line below shows the RXRα-binding sequence. A black line below represents the 5′ extension sequence. WT, wild type.

Materials and Methods

Experimental Animals. All experiments were approved by The Rockefeller University Institutional Animal Care and Use Committee and were performed in accordance with the NIH guidelines. Both male and female mice (>3 wk old) were used for all studies. Mice were housed in a 12-h light/dark cycle with ad libitum access to food and water, except for fasting assays. All mouse lines are either C57BL/6J or FVB/NJ background. Male mice were used for ATAC-seq studies. Male and female mice were used for luciferase studies.

ATAC-Seq. Ten-week-old C57BL/J6 and B6 *ob/ob* male mice were purchased from The Jackson Laboratory. Wild-type mice were fed or fasted for 2 d, and s.c. iWAT was isolated from fasted, fed, and *ob/ob* mice. The fat tissue was minced with blades, dounced in homogenization buffer [20 mM Tricine (pH 7.8), 25 mM D-Sucrose, 15 mM NaCl, 60 mM KCl, 2 mM $MgCl_2$, 0.5 mM spermidine], filtered with an EMD Millipore Nylon-Net Steriflip Vacuum Filter Unit (100 μm), and centrifuged at 18,000 × *g* for 5 min at 4 °C. The resulting nuclei pellet was washed once with tagmentation DNA buffer [10 mM Tris (pH 7.6)·acetic acid, 5 mM $MgCl_2$, 10% dimethylformamide] (49), followed by centrifugation at 500 × *g* for 5 min at 4 °C. After resuspension in the same tagmentation DNA buffer and counting using Trypan blue, an aliquot contacting 50,000 nuclei was performed by means of a transposition reaction using a Nextera DNA Library Preparation Kit (Illumina) and processed as described (22). A library from each mouse was sequenced in one lane using 50-bp × 2 paired-end reads on an Illumina HiSeq 2500 system.

Reads were aligned to the mm9 build and Ensemble gene model (NCBIM37) using Bowtie with parameters: X2000 and –m1. Then, we processed the alignments using Samtools and adjusted the read start sites to represent the center of the transposon-binding event as previously described (22): All reads aligning to the + strand were offset by +4 bp, and all reads aligning to the – strand were offset by –5 bp. Reads in two libraries from two individual mice in each condition were mixed. After that, we found peaks in *ob/ob* samples with at least a threefold higher signal than fasted

conditions using Homer (50). Within the above peak region, footprint scores were calculated based on the Wellington method (51). The conservation score within mammals was downloaded from a University of California, Santa Cruz server and calculated from 20 placental mammal species (52). All of the results were viewed using the Integrative Genomics Viewer (53).

Purification of PPARγ and RXRα. Baculoviruses expressing recombinant FLAG-tagged mouse PPARγ2 (F-mPPARγ2) and human RXRα (F-hRXRα) were prepared as described (54). Sf9 cells were infected with each baculovirus to express the recombinant protein separately, and the soluble extract was prepared by sonication in BC buffer [20 mM Hepes-KOH (pH 7.9), 1 mM EDTA, 10% glycerol, 1 mM DTT, 0.5 mM PMSF] containing 100 mM KCl. After the ultracentrifugation, clear lysate was subjected to HiTrap-Q (GE Healthcare), and bound proteins were eluted using a linear gradient of KCl. PPARγ2 and RXRα were eluted from 250 to 300 mM KCl and from 150 to 200 mM KCl, respectively. PPARγ2 or RXRα was further purified by M2-agarose (Sigma) in BC buffer containing 300 mM KCl, 0.1% Nonidet P-40, and 0.25 mM DTT, and eluted by 0.15 mg/mL triple-FLAG peptide (Sigma).

EMSA. EMSA was performed using the LICOR Odyssey EMSA Buffer Kit. Basically, purified PPARγ (10 ng) and RXRα (10 ng) were incubated in a 20-μL reaction volume with 5 mM Tris (pH 7.5), 25 mM KCl, 3 mM DTT, 0.25% Tween 20, 5 mM $MgCl_2$, 1 μg of poly(dI-dC) (or 0.5 μg of salmon sperm DNA) ,and 2.5 nM IRDye 700-labeled DNA probe, with or without 500 nM unlabeled oligos for 20 min at room temperature. Samples were then mixed with 2 μL of 10× LICOR orange loading dye and loaded onto a 5% Mini-PROTEAN TBE Gel (BioRad). After an ∼75-min run at 70 V, the gel was scanned with a LICOR Odyssey CLx Imaging System. The results were analyzed and quantified with Image Studio Lite (LICOR). The sequences of the IRDye 700-labeled and unlabeled oligos are shown in *SI Appendix*, Table S1. All oligos in this paper were ordered from Integrated DNA Technologies, Inc.

Plasmids. pTK-Renilla luciferase encoded the Renilla luciferase gene under control of the thymidine kinase promoter (Promega). pCMV-PPARγ encoded the mouse PPARγ2 under control of the CMV promoter (54). pCMV-RXRα encoded FLAG-tagged human RXRα under control of the CMV promoter (54). pLE1-firefly luciferase was generated by cloning 115 bp of LE1 (GAGAACACTTAACAGCAAAGGTTAATCTTTGAAGTCCCTAAAGATTTGAACTTTCCGCAGAATTGGCTGCAGCGTCTAGTGGGTTAGAGTCTAATTGGAGTAGAGCAGAAGCAAG) into pGL4.27 (Promega) between the XhoI and HindIII sites. pLE2-firefly luciferase was generated by cloning 279 bp of LE2 (TGGAGGGGCTTTTGGAGAGCTGTTTGTGTGTGACAGGGCAAGGCCTGGCTGGCGTCCAGCCATCACCAGGGTCAGCCCCACCCGGGCTTGGCCACAGCCAGCTACCAGTTATTCAGGCGAAAGGATTACCCTAAGCCCAGGGCCAGGCAAGAAGCAAATTCTACACCAGCGGCTGAGCAGTTCTGCAAACCAGCCTCGAGAAGCACCCAGTTATTTTAAAGCCAGAGTATCAAAACCCCAAGCAAATAACCAAACCCAAACCTCACAGTCTAATGGCA) into pGL4.27 (Promega) between the BglII and HindIII sites.

Dual-Luciferase Reporter Assay. The reporter assay was performed as described elsewhere (55, 56). On day 0, HEK293T cells were set up for experiments in 0.5 mL of DMEM (10-013-CV; Corning) supplemented with 10% FBS (16000044; Thermo Fisher Scientific) at a density of 30,000 cells per well in 24-well plates. On day 1, cells were cotransfected with 0.125 ng of pTK-Renilla luciferase, 12.5 ng of pLE1-firefly luciferase or pLE2-firefly luciferase, 162.7 ng of pCMV-PPARγ, and 162.7 ng of pCMV-RXRα. Fugene 6 was used as the transfection agent. For each transfection, the total amount of DNA was adjusted to 338 ng per dish by the addition of pcDNA mock vector. On day 2, the cells were treated with 1 μM rosiglitazone (Sigma) in DMSO, 1 μM 9-*cis*-Retinoic acid (Sigma–Aldrich) in DMSO, or DMSO alone. On day 3, the cells were washed with PBS, after which luciferase activity was read on a CLARIOstar (BMG Labtech) using the Dual-Luciferase Reporter Assay System (Promega). The amount of LE1 (or LE2) luciferase activity in each dish was normalized to the amount of Renilla luciferase activity in the same dish. A relative luciferase activity of 1 represents the normalized luciferase value in dishes transfected with pcDNA mock vector with DMSO treatment. All values are the average of duplicate assays.

BAC Modification. Recombineering was performed as previously described (57) on a BAC containing −22 to +8.8 kb of leptin-luciferase reporter construct (18). Sequences of primers for creating mutations are included in *SI Appendix*, Table S1. Genomic sequences and coordinates were based on the NCBI37/mm9 mouse genome.

Transgenic Animals. Leptin-luciferase reporter BACs were used to generate transgenic animals in the inbred FVB N/J background (The Jackson Laboratory) using common pronuclear injection techniques (17, 58). B6 *ob*/$^{+}$ mice (The Jackson Laboratory) were crossed to FVB N/J mice (The Jackson Laboratory) for many generations to generate fully inbred FVB *ob*/$^{+}$ mice. Leptin-luciferase reporter BAC transgenic animals were mated with the above FVB *ob*/$^{+}$ mice to produce FVB *ob*/$^{+}$ and FVB *ob*/*ob* transgenic animals.

In Vivo Luciferase Imaging. Fifty microliters of 15 mg/mL XenoLight D-Luciferin (PerkinElmer) in 1× Dulbecco's phosphate-buffered saline was injected i.p. into awake mice. After mice were anesthetized with isoflurane, sequential images were taken with an IVIS Spectrum In Vivo Imaging System (PerkinElmer) until the luciferase intensity passed the highest point. Imaging was normally performed within 15 min after luciferin injection. The photon image was later analyzed by Living Image 4.5 software (PerkinElmer). The image of the highest luciferase intensity was chosen for further analysis.

In Vitro Luciferase Assay. Tissues were harvested and homogenized using a POLYTRON PT 1200E Handheld Homogenizer. After centrifugation at 20,000 × *g* for 10 min at 4 °C, the supernatant was loaded to a 96-well plate and measured using a CLARIOstar microplate reader (BMG Labtech). We used a Luciferase Reporter Assay System (Promega) for the luciferase assay and a DC Protein Assay (BioRad) for protein concentration measurement.

Quantification and Statistical Analysis. Mean values are accompanied by SEM. Statistical parameters, including the sample size (n = number of animals or samples per group), precision measures (mean ± SEM), and statistical significance are reported in the figures and figure legends. A two-ended, unpaired Student's t test was used. Significance was defined as $P < 0.05$. Significance annotations are as follows: $^{*}P < 0.05$, $^{**}P < 0.01$, $^{***}P < 0.001$, and $^{****}P < 0.0001$. Mice were randomized into control or treatment groups. Control mice were age-matched littermate controls where possible. All statistics and data analysis were performed using GraphPad Prism 7.

Data Resources. The ATAC-seq data generated in this publication can be found online associated with Gene Expression Omnibus database accession no. GSE113413.

ACKNOWLEDGMENTS. We thank Kivanc Birsoy, Paul Cohen, Henrik Molina, Sohail Malik, and Ming Yu for valuable discussions; Kenneth Lay and Elaine Fuchs for help with the LICOR Odyssey CLx imaging system; Wenxiang Hu (University of Pennsylvania) and Chunjie Jiang (University of Pennsylvania) for bioinformatic discussions; Xiaofei Yu for help with cell culture; and the Rockefeller University Genomics Resource Center and Comparative Bioscience Center. This project was supported by funding from the JPB Foundation (Grant CEN 5402133 to J.M.F.) and NIH (Grant R01-DK071900 to R.G.R.). Y.Z. acknowledges support from the Howard Hughes Medical Institute. O.S.D. acknowledges support from a Swedish Research Council Fellowship and a Swedish Medical Research Society Fellowship. M.A.L. acknowledges support from the NIH (Grant R01-DK049780) and the JPB Foundation.

1. Zhang Y, et al. (1994) Positional cloning of the mouse obese gene and its human homologue. *Nature* 372:425–432.
2. Montague CT, et al. (1997) Congenital leptin deficiency is associated with severe early-onset obesity in humans. *Nature* 387:903–908.
3. Friedman JM, Halaas JL (1998) Leptin and the regulation of body weight in mammals. *Nature* 395:763–770.
4. Jéquier E (2002) Leptin signaling, adiposity, and energy balance. *Ann N Y Acad Sci* 967:379–388.
5. Kershaw EE, Flier JS (2004) Adipose tissue as an endocrine organ. *J Clin Endocrinol Metab* 89:2548–2556.
6. Coll AP, Farooqi IS, O'Rahilly S (2007) The hormonal control of food intake. *Cell* 129: 251–262.
7. Schwartz MW, et al. (2017) Obesity pathogenesis: An endocrine society scientific statement. *Endocr Rev* 38:267–296.
8. Florant GL, et al. (2004) Fat-cell mass, serum leptin and adiponectin changes during weight gain and loss in yellow-bellied marmots (Marmota flaviventris). *J Comp Physiol B* 174:633–639.
9. Jernås M, et al. (2006) Separation of human adipocytes by size: Hypertrophic fat cells display distinct gene expression. *FASEB J* 20:1540–1542.
10. Skurk T, Alberti-Huber C, Herder C, Hauner H (2007) Relationship between adipocyte size and adipokine expression and secretion. *J Clin Endocrinol Metab* 92:1023–1033.
11. Südhof TC, Russell DW, Brown MS, Goldstein JL (1987) 42 bp element from LDL receptor gene confers end-product repression by sterols when inserted into viral TK promoter. *Cell* 48:1061–1069.

12. Brown MS, Goldstein JL (1997) The SREBP pathway: Regulation of cholesterol metabolism by proteolysis of a membrane-bound transcription factor. *Cell* 89:331–340.
13. Friedman JM (2009) Leptin at 14 y of age: An ongoing story. *Am J Clin Nutr* 89: 973S–979S.
14. Dynan WS, Tjian R (1983) The promoter-specific transcription factor Sp1 binds to upstream sequences in the SV40 early promoter. *Cell* 35:79–87.
15. Sen R, Baltimore D (1986) Multiple nuclear factors interact with the immunoglobulin enhancer sequences. *Cell* 46:705–716.
16. Mandrup S, Loftus TM, MacDougald OA, Kuhajda FP, Lane MD (1997) Obese gene expression at in vivo levels by fat pads derived from s.c. implanted 3T3-F442A preadipocytes. *Proc Natl Acad Sci USA* 94:4300–4305.
17. Birsoy K, et al. (2008) Cellular program controlling the recovery of adipose tissue mass: An in vivo imaging approach. *Proc Natl Acad Sci USA* 105:12985–12990.
18. Lu YH, Dallner OS, Birsoy K, Fayzikhodjaeva G, Friedman JM (2015) Nuclear factor-Y is an adipogenic factor that regulates leptin gene expression. *Mol Metab* 4:392–405.
19. de la Brousse FC, Shan B, Chen JL (1996) Identification of the promoter of the mouse obese gene. *Proc Natl Acad Sci USA* 93:4096–4101.
20. Mason MM, He Y, Chen H, Quon MJ, Reitman M (1998) Regulation of leptin promoter function by Sp1, C/EBP, and a novel factor. *Endocrinology* 139:1013–1022.
21. Wrann CD, et al. (2012) FOSL2 promotes leptin gene expression in human and mouse adipocytes. *J Clin Invest* 122:1010–1021.
22. Buenrostro JD, Giresi PG, Zaba LC, Chang HY, Greenleaf WJ (2013) Transposition of native chromatin for fast and sensitive epigenomic profiling of open chromatin, DNA-binding proteins and nucleosome position. *Nat Methods* 10:1213–1218.
23. Gesta S, Tseng YH, Kahn CR (2007) Developmental origin of fat: Tracking obesity to its source. *Cell* 131:242–256.
24. Graves RA, Tontonoz P, Spiegelman BM (1992) Analysis of a tissue-specific enhancer: ARF6 regulates adipogenic gene expression. *Mol Cell Biol* 12:1202–1208.
25. Tontonoz P, Hu E, Graves RA, Budavari AI, Spiegelman BM (1994) mPPAR gamma 2: Tissue-specific regulator of an adipocyte enhancer. *Genes Dev* 8:1224–1234.
26. Tontonoz P, Hu E, Spiegelman BM (1994) Stimulation of adipogenesis in fibroblasts by PPAR gamma 2, a lipid-activated transcription factor. *Cell* 79:1147–1156.
27. Spiegelman BM (1998) PPAR-gamma: Adipogenic regulator and thiazolidinedione receptor. *Diabetes* 47:507–514.
28. Kliewer SA, Umesono K, Noonan DJ, Heyman RA, Evans RM (1992) Convergence of 9-cis retinoic acid and peroxisome proliferator signalling pathways through heterodimer formation of their receptors. *Nature* 358:771–774.
29. Juge-Aubry C, et al. (1997) DNA binding properties of peroxisome proliferator-activated receptor subtypes on various natural peroxisome proliferator response elements. Importance of the 5′-flanking region. *J Biol Chem* 272:25252–25259.
30. Nielsen R, et al. (2008) Genome-wide profiling of PPARgamma:RXR and RNA polymerase II occupancy reveals temporal activation of distinct metabolic pathways and changes in RXR dimer composition during adipogenesis. *Genes Dev* 22:2953–2967.
31. Lefterova MI, et al. (2008) PPARgamma and C/EBP factors orchestrate adipocyte biology via adjacent binding on a genome-wide scale. *Genes Dev* 22:2941–2952.
32. Soccio RE, et al. (2015) Genetic variation determines PPARγ function and anti-diabetic drug response in vivo. *Cell* 162:33–44.
33. Soccio RE, et al. (2017) Targeting PPARγ in the epigenome rescues genetic metabolic defects in mice. *J Clin Invest* 127:1451–1462.
34. Kallen CB, Lazar MA (1996) Antidiabetic thiazolidinediones inhibit leptin (ob) gene expression in 3T3-L1 adipocytes. *Proc Natl Acad Sci USA* 93:5793–5796.
35. De Vos P, et al. (1996) Thiazolidinediones repress ob gene expression in rodents via activation of peroxisome proliferator-activated receptor gamma. *J Clin Invest* 98: 1004–1009.
36. Zhang B, et al. (1996) Down-regulation of the expression of the obese gene by an antidiabetic thiazolidinedione in Zucker diabetic fatty rats and db/db mice. *J Biol Chem* 271:9455–9459.
37. Krempler F, et al. (2000) Leptin, peroxisome proliferator-activated receptor-gamma, and CCAAT/enhancer binding protein-alpha mRNA expression in adipose tissue of humans and their relation to cardiovascular risk factors. *Arterioscler Thromb Vasc Biol* 20:443–449.
38. Wang F, Mullican SE, DiSpirito JR, Peed LC, Lazar MA (2013) Lipoatrophy and severe metabolic disturbance in mice with fat-specific deletion of PPARγ. *Proc Natl Acad Sci USA* 110:18656–18661.
39. Heery DM, Kalkhoven E, Hoare S, Parker MG (1997) A signature motif in transcriptional co-activators mediates binding to nuclear receptors. *Nature* 387:733–736.
40. Chandra V, et al. (2008) Structure of the intact PPAR-gamma-RXR- nuclear receptor complex on DNA. *Nature* 456:350–356.
41. Lodish HF (2000) *Molecular Cell Biology* (Freeman, New York), 4th Ed.
42. Puigserver P, et al. (1998) A cold-inducible coactivator of nuclear receptors linked to adaptive thermogenesis. *Cell* 92:829–839.
43. Harms MJ, et al. (2015) PRDM16 binds MED1 and controls chromatin architecture to determine a brown fat transcriptional program. *Genes Dev* 29:298–307.
44. Emmett MJ, et al. (2017) Histone deacetylase 3 prepares brown adipose tissue for acute thermogenic challenge. *Nature* 546:544–548.
45. Weikum ER, Knuesel MT, Ortlund EA, Yamamoto KR (2017) Glucocorticoid receptor control of transcription: Precision and plasticity via allostery. *Nat Rev Mol Cell Biol* 18: 159–174.
46. Lam TK, Schwartz GJ, Rossetti L (2005) Hypothalamic sensing of fatty acids. *Nat Neurosci* 8:579–584.
47. Wang X, et al. (1993) Nuclear protein that binds sterol regulatory element of low density lipoprotein receptor promoter. II. Purification and characterization. *J Biol Chem* 268:14497–14504.
48. Brown MS, Radhakrishnan A, Goldstein JL (2017) Retrospective on cholesterol homeostasis: The central role of scap. *Annu Rev Biochem*, 10.1146/annurev-biochem-062917-011852.
49. Wang Q, et al. (2013) Tagmentation-based whole-genome bisulfite sequencing. *Nat Protoc* 8:2022–2032.
50. Heinz S, et al. (2010) Simple combinations of lineage-determining transcription factors prime cis-regulatory elements required for macrophage and B cell identities. *Mol Cell* 38:576–589.
51. Piper J, et al. (2013) Wellington: A novel method for the accurate identification of digital genomic footprints from DNase-seq data. *Nucleic Acids Res* 41:e201.
52. Murphy WJ, et al. (2001) Resolution of the early placental mammal radiation using Bayesian phylogenetics. *Science* 294:2348–2351.
53. Thorvaldsdóttir H, Robinson JT, Mesirov JP (2013) Integrative genomics viewer (IGV): High-performance genomics data visualization and exploration. *Brief Bioinform* 14: 178–192.
54. Wallberg AE, Yamamura S, Malik S, Spiegelman BM, Roeder RG (2003) Coordination of p300-mediated chromatin remodeling and TRAP/mediator function through coactivator PGC-1alpha. *Mol Cell* 12:1137–1149.
55. Zhang Y, Motamed M, Seemann J, Brown MS, Goldstein JL (2013) Point mutation in luminal loop 7 of scap protein blocks interaction with loop 1 and abolishes movement to Golgi. *J Biol Chem* 288:14059–14067.
56. Jiang H, et al. (2013) Regulation of transcription by the MLL2 complex and MLL complex-associated AKAP95. *Nat Struct Mol Biol* 20:1156–1163.
57. Gong S, et al. (2003) A gene expression atlas of the central nervous system based on bacterial artificial chromosomes. *Nature* 425:917–925.
58. Behringer R, Gertsenstein M, Vintersten Nagy K, Nagy A, Nagy KV (2013) *Manipulating the Mouse Embryo: A Laboratory Manual* (Cold Spring Harbor Lab Press, Cold Spring Harbor, NY), 4th Ed.